$R = V_d/V_c$
$r = (\rho C_p)_d/(\rho C_p)_c$
S = defined by Equation (20)
t = temperature, °C.
V = superficial velocity of liquid, cc./(sq. cm.)(sec.)
v_D = volume of drop, cc.
z = distance along wake shedding zone, cm.

Greek Letters

α = defined by Equation (19), cm.$^{-1}$
θ = dimensionless concentration
Θ_b = defined by Equation (24)
ρ = density, g./cc.

Subscripts

c = continuous phase
d = dispersed phase
i = at inlet
l = at top of wake shedding zone
o = at outlet
s = at bottom of wake shedding zone
w = wake
z = at any point along the wake shedding zone

Superscript

* = at equilibrium

LITERATURE CITED

1. Appel, F. J., and J. C. Elgin, *Ind. Eng. Chem.*, **29**, 451 (1937).
2. Baird, M. H. I., M. G. Senior, and R. J. Thompson, *Chem. Eng. Sci.*, **22**, 551 (1967).
3. Cavers, S. D., and J. E. Ewanchyna, *Can. J. Chem. Eng.*, **35**, 113 (1957).
4. Crittendon, E. D., and A. N. Hixon, *Ind. Eng. Chem.*, **46**, 265 (1954).
5. Elgin, J. C., and F. M. Browning, *Trans. Am. Inst. Chem. Eng.*, **31**, 639 (1935).
6. Fleming, J. F., and H. F. Johnson, *Chem. Eng. Progr.*, **49**, 497 (1953).
7. Garner, F. H., and M. Tayeban, *Anales Real Soc. Espan. Fis. Quim. Ser. B*, **56**, 479 (1960).
8. Geankoplis, C. J., and A. N. Hixon, *Ind. Eng. Chem.*, **42**, 1141 (1951).
9. Geankoplis, C. J., P. L. Wells, and E. L. Hawk, *ibid.*, **43**, 1848 (1951).
10. Gier, T. E., and J. O. Hougen, *ibid.*, **45**, 1362 (1953).
11. Hanson, Carl, *Chem. Eng.*, **75**(18), 76 (1968).
12. Hendrix, C. D., S. B. Dave, and H. F. Johnson, *AIChE J.*, **13**, 1072 (1967).
13. Johnson, H. F., and Harding Bliss, *Trans. Am. Inst. Chem. Eng.*, **42**, 331 (1946).
14. Kreager, R. M., and C. J. Geankoplis, *Ind. Eng. Chem.*, **45**, 2156 (1953).
15. Kylander, R. L., and L. Garwin, *Chem. Eng. Progr.*, **47**, 186 (1951).
16. Laddha, G. S., and J. M. Smith, *ibid.*, **46**, 195 (1950).
17. Letan, Ruth, and Ephraim Kehat, *AIChE J.*, **11**, 804 (1965).
18. *Ibid.*, **13**, 443 (1967).
19. *Ibid.*, **14**, 398 (1968).
20. *Ibid.*, **16**, 955 (1970).
21. Magarvey, R. H., and R. L. Bishop, *Can. J. Phys.*, **39**, 1418 (1961).
22. Magarvey, R. H., and C. S. MacLatchy, *AIChE J.*, **14**, 260 (1968).
23. Morello, V. S., and N. Poffenberger, *Ind. Eng. Chem.*, **42**, 1201 (1950).
24. Perry, J. H., ed., "Chemical Engineering Handbook," 4th edit., pp. 14–15, McGraw-Hill, New York (1963).
25. Row, S. B., J. H. Koffolt, and J. R. Withrow, *Trans. Am. Inst. Chem. Eng.*, **37**, 559 (1941).
26. Ruby, C. L., and J. C. Elgin, *Chem. Eng. Progr. Symp. Ser. No. 16*, **51**, 17 (1955).
27. Seidell, A., "Solubilities of Organic Compounds," 3rd edit., Vol. 2, p. 112, Van Nostrand, New York (1941).
28. Sherwood, T. K., J. E. Evans, and J. V. A. Longcor, *Ind. Eng. Chem.*, **31**, 1144 (1939).
29. Shih, C., and R. R. Kraybill, *Ind. Eng. Chem. Process Design Develop.*, **5**, 260 (1966).
30. Vogt, H. J., and C. J. Geankoplis, *Ind. Eng. Chem.*, **45**, 2219 (1953).
31. *Ibid.*, **46**, 1763 (1954).
32. Winnikow, S., and B. T. Chao, *Phys. Fluids*, **9**, 50 (1966).

Manuscript received March 27, 1969; revision received August 25, 1969; paper accepted August 29, 1969.

Turbulent Flow of Dilute Polymer Solutions Through an Annulus

HILLEL RUBIN and CHAIM ELATA

Israel Institute of Technology, Haifa, Israel

A semiempirical analysis of the turbulent flow of dilute polymer solutions through an annulus between two coaxial tubes is presented. This analysis is based upon the assumption that the velocity profile is logarithmic in the turbulent region. The thickness of the laminar boundary sublayer is changed by adding polymers to the solvent; this change is different at each wall of the annulus. A series of experiments was conducted in an annular system. The experimental results fit the theoretical predictions quite well.

Axial flow between concentric tubes is often encountered in heat exchangers in which heat is transferred between two fluids flowing turbulently through the annular space and the inner tube.

Major changes in the characteristics of turbulent flow may be effected by adding minute quantities of high molecular polymers to a liquid. This phenomenon, which has been studied recently in turbulent pipe flow, may also generate drastic changes in the characteristics of annular flow. The potential practical importance of this phenomenon has led us to investigate the turbulent flow of dilute polymer solutions in a concentric smooth annulus.

Laminar flow in an annulus may be described by an exact solution of the Navier-Stokes equations; turbulent flow in an annulus was little investigated until several years ago.

The analysis of annular flow proposed by Meter and Bird (*1*) is based on the assumptions that the local mean velocity profile is logarithmic and that the location of the maximum local mean velocity in the cross section is the same as in a laminar and turbulent flow. Expressions for the relation between friction factor and Reynolds number were obtained on the basis of these assumptions.

Barrow, Lee, and Roberts (*2*) pointed out that the turbulent flow resembles that in pipes in the outer region of an annulus, but not in the inner one. They based their analysis on earlier work by Goldstein (*3*).

Macagno and McDougall (*4*), as Meter and Bird (*1*), assumed a logarithmic local mean velocity profile, but did not think that the locations of the maximum velocities in laminar and turbulent flow coincide. By assuming continuity of the velocity profile at the location of maximum velocity, they obtained expressions for the velocity profile and the friction factor. Macagno and McDougall found good correlation between their theory and experimental results for Reynolds numbers higher than 7×10^3.

In the following analysis of annular flow of dilute polymer solutions, we have adapted Macagno et al.'s basic assumptions for the sake of convenience. The reduction of friction losses in flow with polymeric additives has been described semi-empirically in two ways: (1) On the basis of the ratio of the characteristic time of the turbulent shear flow near the wall and a characteristic relaxation time of the coiling polymer (*5* to *7*). (2) On the basis of the ratio of the characteristic length of the turbulent shear flow near the wall and a characteristic length of the polymer molecules (*8*, *9*). Considerable controversy exists between the proponents of each of these approaches. The present analysis will present the results of calculations based on both. These calculations will be compared with the results of a series of experiments.

THEORY

Let us assume that two coaxial tubes create an annulus with an inner radius r_1 and an outer radius r_2 (Figure 1). The maximum local mean velocity of the flow in the annulus is located at a distance r_0 from the axis.

We define

$$\beta_1 = \frac{r_1}{r_2}; \quad \beta_0 = \frac{r_0}{r_2} \tag{1}$$

The shear stress near the inner wall is τ_{w_1} and near the outer wall τ_{w_2}; the mean shear stress over the cross section is τ_{w_a}. Using the geometrical considerations and the assumption that $\tau_w = 0$ at $r = r_0$, one may write

$$\frac{\tau_{w_1}}{\tau_{w_2}} = \frac{1}{\beta_1} \frac{\beta_0^2 - \beta_1^2}{1 - \beta_0^2} \tag{2}$$

$$\tau_{w_a} = \frac{\beta_1 \tau_{w_1} + \tau_{w_2}}{1 + \beta_1} \tag{3}$$

The flow in the cross section may be regarded as consisting of two separate major regions: the inner region ($r_1 < r < r_0$) and the outer region ($r_0 < r < r_2$).

In annular flow we may define three different Darcy-Weissbach coefficients of friction as follows:

$$f_a = \frac{8\tau_{w_a}}{\rho V_a^2}; \quad f_1 = \frac{8\tau_{w_1}}{\rho V_1^2}; \quad f_2 = \frac{8\tau_{w_2}}{\rho V_2^2} \tag{4}$$

Where f_a, V_a, f_1, V_1 and f_2, V_2 are the friction factor and mean velocity over the whole cross section, the inner and the outer regions, respectively.

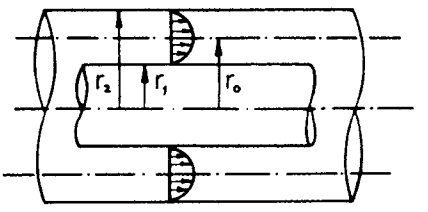

Fig. 1. Description of annular flow.

The Reynolds number for annular flow is defined by

$$N_{Re} = \frac{2V_a r_2 (1 - \beta_1)}{\nu} \tag{5}$$

where ν is the kinematic viscosity of the liquid.

Each one of the two prime regions is divided into three subregions (Figure 2) as follows:

1. Laminar boundary sublayer. In this region the velocity distribution is assumed to be linear.

$$u^+ = y^+ \tag{6}$$

where

$$u^+ = \frac{u}{\sqrt{\tau_w/\rho}}; \quad y^+ = \frac{y\sqrt{\tau_w/\rho}}{\nu} \tag{7}$$

2. The buffer zone. In this region the flow is influenced by viscous as well as inertial forces. This is the major region in which the creation and decay of turbulent vortices take place. According to von Karman, the distribution of local mean velocities in this region is

$$u^+ = \delta^+ \ln \frac{y^+}{\delta^+} + \delta^+ \tag{8}$$

where δ is the thickness of the laminar sublayer. For Newtonian fluids $\delta \approx 5$.

3. The fully developed turbulent region. In this region the local mean velocity profile is also logarithmic, and may be expressed for Newtonian liquids by

$$u^+ = \frac{1}{k} \ln \frac{y^+}{11.6} + 11.6 \tag{9}$$

where k is von Karman's universal constant equal to 0.4.

Analysis According to the "Characteristic Times" Approach

According to Elata et al. (*6*) dissolved polymeric molecules may influence the vortices in turbulent flow when their maximal relaxation time (t_1) is at least of the same order of magnitude as the minimal characteristic time of the turbulent vortices (η/τ_w). In this case the polymeric molecules may decrease the high frequency velocity fluc-

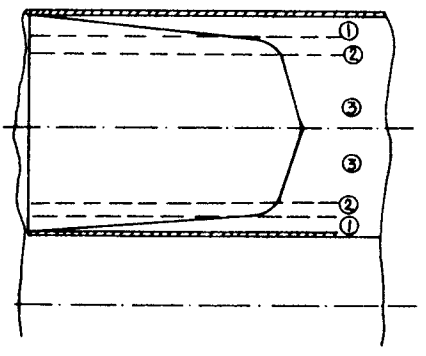

Fig. 2. Three regions in the turbulent annular flow. 1, Laminar sublayer. 2, Transition zone. 3, Developed turbulent zone.

tuations, which increases the thickness of the laminar boundary sublayer.

From these assumptions Elata et al. (6) deduced that the velocity profile for the flow of dilute polymer solutions in the fully developed turbulent region is

$$u^+ = \frac{1}{k} \ln \frac{y^+}{11.6} + 11.6 + \Delta u^+ \tag{10}$$

where

$$\Delta u^+ = \frac{A}{k} \ln \frac{\tau_w t_1}{\eta} \tag{11}$$

Here η is the viscosity, A is a function of the concentration, and t_1 is the maximum relaxation time of the polymer solution calculated according to the theories of Rouse (10) or Zimm (11). According to Rouse (10)

$$t_1 = \frac{\eta_0 (\eta_{sp}/c) M}{1.64 R \theta}$$

Reduction of frictional forces only occurs when the characteristic time of the polymer (t_1) is larger than the characteristic time of the turbulent shear near the wall (η/τ_w).

Equation (10) applies therefore only when $\tau_w t_1/\eta > 1$. For the case in which $\tau_w t_1/\nu \leq 1$, no changes occur in the velocity profile.

In the case of annular flow we may write for the inner and outer turbulent regions, respectively

$$u_1^+ = \frac{1}{k} \ln y_1^+ + 5.5 + \Delta u_1^+$$
$$u_2^+ = \frac{1}{k} \ln y_2^+ + 5.5 + \Delta u_2^+ \tag{12}$$

From the continuity of the velocity profile at r_0 one may obtain from Equations (12)

$$\sqrt{\frac{\tau_{w_2}}{\tau_{w_1}}} = \frac{\frac{1}{k} \ln \left(\sqrt{\frac{\tau_{w_1}}{\rho}} \frac{r_0 - r_1}{\nu} \right) + 5.5 + \Delta u_1}{\frac{1}{k} \ln \left(\sqrt{\frac{\tau_{w_2}}{\rho}} \frac{r_2 - r_0}{\nu} \right) + 5.5 + \Delta u_2^+} \tag{13}$$

or

$$\left[\frac{\beta_1 (1 - \beta_0^2)}{\beta_0^2 - \beta_1^2} \right]^{1/2} = \frac{\ln \left[\frac{N_{Re} \sqrt{f_a}}{4\sqrt{2}} \left(\frac{\beta_0^2 - \beta_1^2}{\beta_1 (1 - \beta_1)} \right)^{1/2} \frac{\beta_0 - \beta_1}{1 - \beta_1} \right] + 2.2 + A \ln \left[N_{Re}^2 f_a T \frac{\beta_0^2 - \beta_1^2}{\beta_1 (1 - \beta_1)} \right]}{\ln \left[\frac{N_{Re} \sqrt{f_a}}{4\sqrt{2}} \left(\frac{1 - \beta_0^2}{1 - \beta_1} \right)^{1/2} \frac{1 - \beta_0}{1 - \beta_1} \right] + 2.2 + A \ln \left[N_{Re} f_a T \frac{1 - \beta_0^2}{1 - \beta_1} \right]} \tag{14}$$

where

$$T = \frac{t_1 \nu}{32 r_2^2 (1 - \beta_1)^2} \tag{15}$$

In Equation (14) terms which are multiplied by A will not appear unless the corresponding natural logarithm is greater than 0. Without these terms Equation (14) expresses the relation between β_0, N_{Re}, $\sqrt{f_a}$, and β_1 for Newtonian liquids. For polymer solution β_0 depends also on the type of polymer (t_1), the concentration of the solution (A), and on a characteristic length of the annulus (r_2).

The rate of flow through the annulus may be found by integrating the velocity profile over the cross section. In this way equations are derived which show the relations between the coefficients of friction and Reynolds number as follows:

$$\frac{1}{\sqrt{f_a}} = \frac{5}{2\sqrt{2}(1 - \beta_1^2)} \left(\frac{\beta_0^2 - \beta_1^2}{\beta_1 (1 - \beta_1)} \right)^{1/2} \left\{ \left(\frac{\beta_0^2 - \beta_1^2}{2} \right) \left[\ln \left(\frac{N_{Re} \sqrt{f_a}}{4\sqrt{2}} \left(\frac{\beta_0^2 - \beta_1^2}{\beta_1 (1 - \beta_1)} \right)^{1/2} \frac{\beta_0 - \beta_1}{1 - \beta_1} \right) + 2.2 + A \ln \left(N_{Re}^2 f_a T \frac{\beta_0^2 - \beta_1^2}{\beta_1 (1 - \beta_1)} \right) \right] - \frac{(\beta_1 + \beta_0)^2}{4} + \beta_1^2 \right\}$$
$$+ \frac{5}{2\sqrt{2}(1 - \beta_1^2)} \left(\frac{1 - \beta_0^2}{1 - \beta_1} \right)^{1/2} \left\{ \left(\frac{1 - \beta_0^2}{2} \right) \left[\ln \left(\frac{N_{Re} \sqrt{f_a}}{4\sqrt{2}} \left(\frac{1 - \beta_0^2}{1 - \beta_1} \right)^{1/2} \frac{1 - \beta_0}{1 - \beta_1} \right) + 2.2 + A \ln \left(N_{Re}^2 f_a T \frac{1 - \beta_0^2}{1 - \beta_1} \right) \right] + \frac{(\beta_0 + 1)^2}{4} - 1 \right\} \tag{16}$$

$$\frac{1}{\sqrt{f_1}} = \frac{5}{2\sqrt{2}(\beta_0^2 - \beta_1^2)} \left\{ \left(\frac{\beta_0 - \beta_1^2}{2} \right) \left[\ln \left(\frac{N_{Re} \sqrt{f_a}}{4\sqrt{2}} \left(\frac{\beta_0^2 - \beta_1^2}{\beta_1 (1 - \beta_1)} \right)^{1/2} \frac{1 - \beta_0}{1 - \beta_1} \right) + 2.2 + A \ln \left(N_{Re}^2 f_a T \frac{\beta_0^2 - \beta_1^2}{\beta_1 (1 - \beta_1)} \right) \right] - \frac{(\beta_1 + \beta_0)^2}{4} + \beta_1^2 \right\} \tag{17}$$

$$\frac{1}{\sqrt{f_2}} = \frac{5}{2\sqrt{2}(1 - \beta_0^2)^2} \left\{ \left(\frac{1 - \beta_0^2}{2} \right) \left[\ln \left(\frac{N_{Re} \sqrt{f_a}}{4\sqrt{2}} \left(\frac{1 - \beta_0^2}{1 - \beta_1} \right)^{1/2} \frac{1 - \beta_0}{1 - \beta_1} \right) + 2.2 + A \ln \left(N_{Re}^2 f_a T \frac{1 - \beta_0^2}{1 - \beta_1} \right) \right] + \frac{(\beta_0 + 1)^2}{4} - 1 \right\} \tag{18}$$

The local mean velocity profile and the relationship between the friction factors and Reynolds number may be obtained by assuming values for $N_{Re} \sqrt{f_a}$. By iteration the magnitude of β_0 is found from Equation (14). The relationship between the friction factors and Reynolds number can be obtained from Equations (16), (17), and (18). We can distinguish between three possible types of flow.

No reduction in frictional drag is attained:

$$\left(\frac{\tau_{w_1} t_1}{\eta} < 1; \quad \frac{\tau_{w_2} t_1}{\eta} < 1 \right)$$

Drag reduction occurs either at the inner wall:

$$\left(\frac{\tau_{w_2} t_1}{\eta} > 1 \right) \text{ or at the outer wall } \left(\frac{\tau_{w_2} t_1}{\eta} > 1 \right)$$

Friction is reduced at both walls:

$$\left(\text{both } \frac{\tau_{w_1} t_1}{\eta} > 1 \quad \text{and} \quad \frac{\tau_{w_2} t_1}{\eta} > 1\right)$$

According to the above formulation, friction is reduced at the inner wall when

$$N_{Re}^2 f_a T \frac{\beta_0 - \beta_1}{\beta_1(1 - \beta_1)} > 1 \tag{19}$$

and at the outer wall when

$$N_{Re}^2 f_a T \frac{1 - \beta_0^2}{1 - \beta_1} > 1 \tag{20}$$

Analysis According to the "Characteristic Lengths" Approach

Virk et al. (*8*) have suggested that the reduction of friction loss and the "threshold" Reynolds number at which frictional drag reduction starts can best be described by characteristic lengths.

According to van-Driest (*9*), the characteristic length of the polymer molecule is a multiple of its mean diameter. The characteristic length of the turbulent flow is the wave length of the turbulent vortices at the region of the maximum dissipation assumed to be given by $\nu\sqrt{\tau_w/\rho}$.

According to van Driest, the turbulent Newtonian flow may be divided into two regions: the viscous sublayer near the boundary of the conduit and the developed turbulent region. In the viscous zone the velocity varies linearly according to Equation (6), while in the turbulent region the velocity profile is logarithmic according to Equation (9). The thickness of the laminar sublayer is given by $\delta^+ \approx 11.6$.

By adding polymers to the solvent, a third intermediate region is created in which the polymer molecules, acting as a grid, change the dimensions of the turbulent vortices. This region is created only when $\delta^+ < L^+$. The velocity distribution in this intermediate region is again logarithmic

$$u^+ = 11.6 + \frac{1}{k'} \ln \frac{y^+}{11.6} \tag{21}$$

but k', the constant of von Karman, is modified. For $L^+ < 11.6$, there is no grid region and $k' = k = 0.4$. If $L^+ > 11.6$, the magnitude of k' can be found from the expression

$$k' = k\left\{1 - \frac{c}{B}\left[1 - \exp\left(-\frac{B}{c}\right)\right]\right\} \tag{22}$$

where B depends upon the type of polymer molecules and c is their concentration.

From the continuity of the velocity profile at r_0 we obtain, similar to Equation (14)

$$\left[\frac{\beta_1(1 - \beta_0^2)}{\beta_0^2 - \beta_1^2}\right]^{1/2} = \frac{11.6 + \frac{1}{k'} \ln\left[\frac{N_{Re}\sqrt{f_a}}{46.4\sqrt{2}} \left(\frac{\beta_0^2 - \beta_1^2}{\beta_1(1 - \beta_1)}\right)^{1/2} \frac{\lambda}{1 - \beta_1}\right] + 2.5 \ln\left(\frac{\beta_0 - \beta_1}{\lambda}\right)}{11.6 + \frac{1}{k'} \ln \frac{N_{Re}\sqrt{f_a}}{46.4\sqrt{2}} \left(\frac{1 - \beta_0^2}{1 - \beta_1}\right)^{1/2} \frac{\lambda}{1 - \beta_1}\Big] + 2.5 \ln\left(\frac{1 - \beta_0}{\lambda}\right)} \tag{23}$$

where

$$\lambda = \frac{L}{r_2} \tag{24}$$

By the integration of the velocity profile the friction coefficients are obtained as follows:

$$\frac{1}{\sqrt{f_a}} = \frac{5}{2\sqrt{2}(1 - \beta_1^2)}\left[\frac{\beta_0^2 - \beta_1^2}{\beta_1(1 - \beta_1)}\right]^{1/2}\left\{\left(\frac{\beta_0^2 - \beta_1^2}{5}\right)\left[11.6 + \frac{1}{k'} \ln\left(\frac{N_{Re}\sqrt{f_a}}{46.4\sqrt{2}}\left(\frac{\beta_0^2 - \beta_1^2}{\beta_1(1 - \beta_1)}\right)^{1/2} \frac{\lambda}{1 - \beta_1}\right) + 2.5 \ln\left(\frac{\beta_0 - \beta_1}{\lambda}\right)\right]\right.$$
$$\left. - \frac{(\beta_0 + \beta_1)^2}{4} + \beta_1^2\right\} + \frac{5}{2\sqrt{2}(1 - \beta_1^2)}\left[\frac{1 - \beta_0^2}{1 - \beta_1}\right]^{1/2}\left\{\left(\frac{1 - \beta_0^2}{5}\right)\left[11.6 + \frac{1}{k'} \ln\left(\frac{N_{Re}\sqrt{f_a}}{46.4\sqrt{2}}\left(\frac{1 - \beta_0^2}{1 - \beta_1}\right)^{1/2} \frac{\lambda}{1 - \beta_1}\right)\right.\right. \tag{25}$$
$$\left.\left. + 2.5 \ln\left(\frac{1 - \beta_0}{\lambda}\right)\right] + \frac{(1 - \beta_0)^2}{4} - 1\right\}$$

$$\frac{1}{\sqrt{f_1}} = \frac{5}{2\sqrt{2}(\beta_0^2 - \beta_1^2)}\left\{\left(\frac{\beta_0^2 - \beta_1^2}{5}\right)\left[11.6 + \frac{1}{k'} \ln\left(\frac{N_{Re}\sqrt{f_a}}{46.4\sqrt{2}}\left(\frac{\beta_0^2 - \beta_1^2}{\beta_1(1 - \beta_1)}\right)^{1/2} \frac{\lambda}{1 - \beta_1}\right) + 2.5 \ln\left(\frac{\beta_0 - \beta_1}{\lambda}\right)\right] - \frac{(\beta_0 + \beta_1)^2}{4} + \beta_1^2\right\} \tag{26}$$

$$\frac{1}{\sqrt{f_2}} = \frac{5}{2\sqrt{2}(1 - \beta_0^2)}\left\{\left(\frac{1 - \beta_0^2}{5}\right)\left[11.6 + \frac{1}{k'} \ln\left(\frac{N_{Re}\sqrt{f_a}}{46.4\sqrt{2}}\left(\frac{1 - \beta_0^2}{1 - \beta_1}\right)^{1/2} \frac{\lambda}{1 - \beta_1}\right) + 2.5 \ln\left(\frac{1 - \beta_1}{\lambda}\right)\right] + \frac{(1 + \beta_0)^2}{4} - 1\right\} \tag{27}$$

β_0 can be found from Equation (23) by iteration. The coefficients of friction f_a, f_1, and f_2 can be found from Equations (25), (26), and (27), respectively.

Frictional drag reduction occurs at the inner wall when

$$\frac{N_{Re}\sqrt{f_a}}{46.4\sqrt{2}} \frac{\lambda}{1 - \beta_1}\left(\frac{\beta_0^2 - \beta_1^2}{\beta_1(1 - \beta_1)}\right)^{1/2} > 1 \tag{28}$$

and at the outer wall when

$$\frac{N_{Re}\sqrt{f_a}}{46.4\sqrt{2}} \frac{\lambda}{1 - \beta_1}\left(\frac{1 - \beta_0^2}{1 - \beta_1}\right)^{1/2} > 1 \tag{29}$$

If the above expressions are smaller than unity, the turbulent flow is Newtonian and $k' = k = 0.4$.

Some Preliminary Numerical Calculations

In order to determine relevant design criteria for the experimental system, numerical calculations were made to determine the characteristics of annular flow.

These calculations were based on the characteristics of a guar gum solution which was previously investigated in pipe flow by Elata et al. (*6*).

The results of these pipe flow experiments were already analyzed earlier according to the "characteristic times" approach by Elata et al. (*6*) and according to the "characteristic lengths" approach by van Driest (*9*).

With the polymer parameters A and B determined from the pipe flow data, the calculations showed similar behavior in annular flow as predicted by both approaches. Some of the results are presented in Figures 3 and 4. The slight in-

fluence of Reynolds number on τ_{w_1}/τ_{w_2} is shown in Figure 5.

Still, the fact that the polymer additives change the ratio between the shear stresses at inner and outer walls may be important in heat transfer problems. Annular systems for heat exchange should be designed in such a way that the shear stress at the inner wall is greater than that at the outer wall. In such a system, a reduction of the ratio τ_{w_1}/τ_{w_2}, as would be caused by the introduction of polymer molecules, decreases the heat transfer capability through the inner wall. In general, one may conclude that there are two separate causes for the decrease in heat transfer in an annular system with polymer solutions. The first cause was explained and analyzed by Poreh and Paz (*12*), and is related to the thickening of the laminar sublayer. The second cause, which is typical for annular flow, is related to the shift in the ratio of shear stress as explained above.

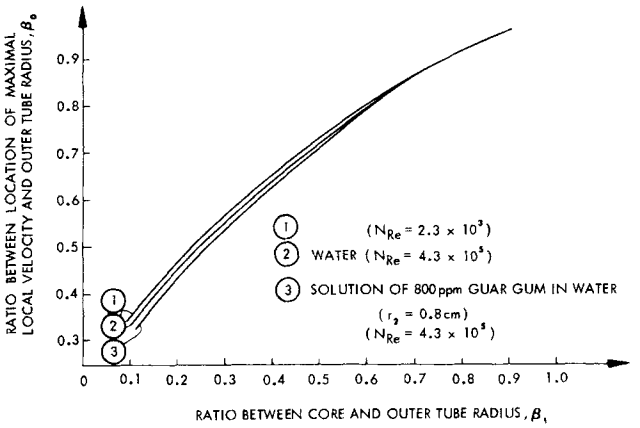

Fig. 3. Computed location of the maximum velocity in the cross section.

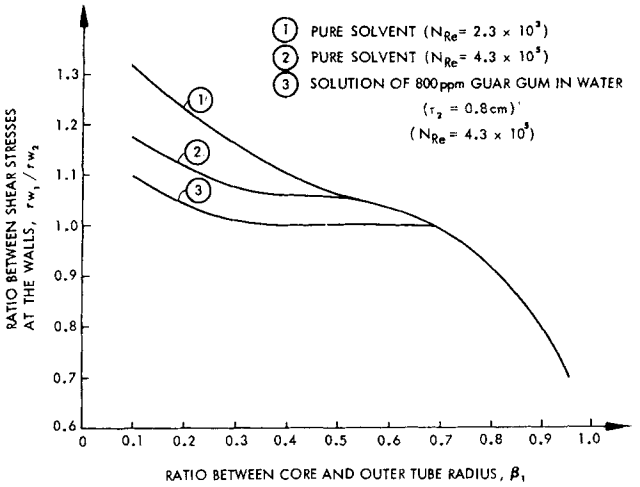

Fig. 4. Computed ratio between shear stresses at the walls as a function of β_1.

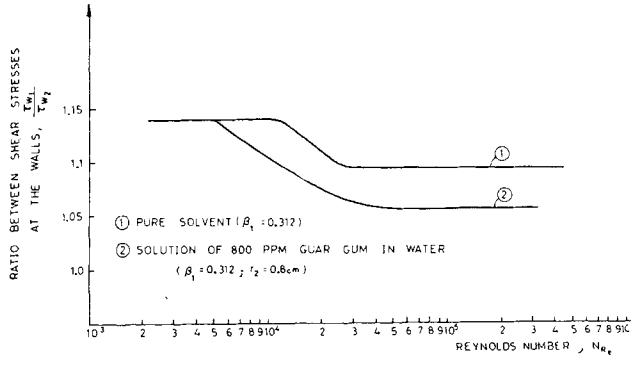

Fig. 5. Computed ratio between shear stresses at the walls as a function of Reynolds number.

EXPERIMENTAL INVESTIGATION

Description of Apparatus and Experiments

The experiments were conducted in a system shown schematically in Figure 6. This system consists of three test sections made of bronze. The first test section has an annular cross section of an I.D. of 5.0 mm., an O.D. of 16.0 mm., and a length of 2,300 mm. The other two test sections are pipes with I.D. of 5.9 and 10.3 mm., and lengths of 860 and 1,200 mm., respectively. The return loop is constructed of a 1¼-in. pipe. A Mono CD-40 pump provides 4,500 liters/hr. against a pressure of 1.5 kg/sq. cm.

The pressure gradient along the test sections was measured by pressure taps consisting of four circumferential holes diametrically opposed and enclosed in a ring to obtain accurate average pressure readings.

The inner core of the annulus was centered by thin supports with an elliptic cross section. The flow rate measurements were conducted by a rotameter (Fischer and Porter) covering the range from 400 to 4,500 liters/hr., which was volumetrically calibrated for each type of solution.

A series of pressure drop and discharge measurements was made along the test sections with solutions in kerosene of EPR (ethylene propylene rubber, manufactured by Hercules, Inc.) at concentrations of 200, 400, and 800 mg./liter. This high molecular weight polymer was found not to degrade. It is therefore suitable for reproducible experiments. Solutions of another polymer, Oppanol B-200 (Polyisobutylene, manufactured by Badische Anilin und Soda Fabrik) were also used, but because of its high degradation, measurements in the annular system were conducted at concentrations of 800 mg./liter only. Analysis of the data indicated that pressure drop and flow rate determinations were obtained with a 2% precision usual in such work.

The viscosities of the solutions were determined by an Ubbelhode capillary viscometer.

Results and Discussion

An approximate value of 4.1×10^5 was found for the molecular weight of EPR determined according to Mooney's viscosity method (*13*), while the molecular weight of Oppanol B-200 was found to be 3.5×10^6 from the intrinsic viscosity of its solutions in cyclohexane (*14*). These determinations led to "effective"

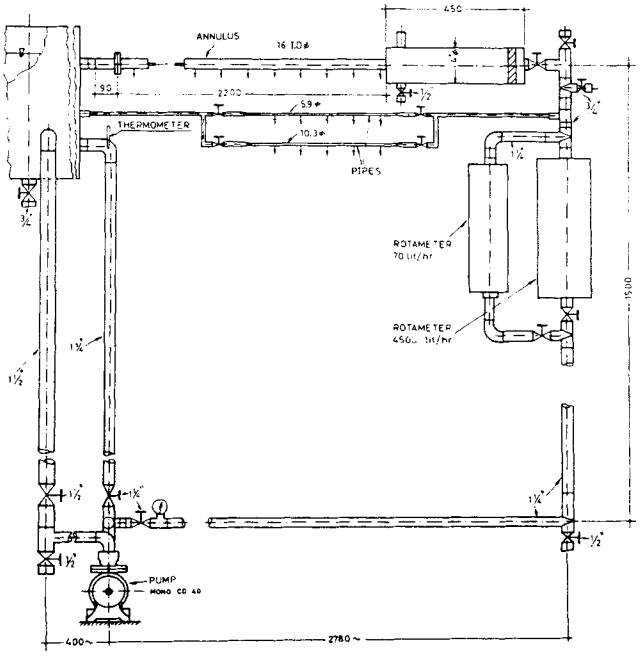

Fig. 6. Experimental system.

molecular weights because of the polydisperse nature of the technical grade polymers used.

Results of the experiments of pipe flow of EPR solutions were plotted in the conventional friction coefficient Reynolds number diagram (Figure 7). Reynolds numbers were based on actual solution—viscosities which, at the concentration used, were found to be shear independent. From the data of Figure 7 the characteristic time of the solution was calculated according to threshold Reynolds numbers data. They were found to be approximately equal to the maximum relaxation time calculated from the crude molecular weight determinations according to molecular theories (*10, 11*). Therefore threshold Reynolds numbers occurred when Deborah numbers (*15*) were equal to unity. The characteristic lengths of the flows which were calculated from threshold Reynolds numbers were approximately equal to a hundred times the length of polymer molecules determined from intrinsic viscosities measurements.

From the data of Figure 7 the constants A and k' were computed. The results are shown in Figures 8 and 9, respectively. It was found that for dilute solutions of EPR in kerosene, the constant A was proportional to the concentration of the solution given by

$$A = 0.35\,c \tag{30}$$

This proportionality between A and c is in agreement with the results of Elata et al. (*6*), which were obtained for guar gum solutions in water.

The constant k' was found to be an exponential function of the concentration

$$k' = 0.4\left\{1 - \frac{c}{270}\left[1 - \exp\left(-\frac{270}{c}\right)\right]\right\}. \tag{31}$$

Such an exponential relationship is in agreement with van Driest's theory (*9*).

The experimental results of the flow of EPR solutions in the annulus system are shown in Figures 10 and 11. The solid lines in these figures were obtained from computations according to the characteristic times and the characteristic lengths approaches,

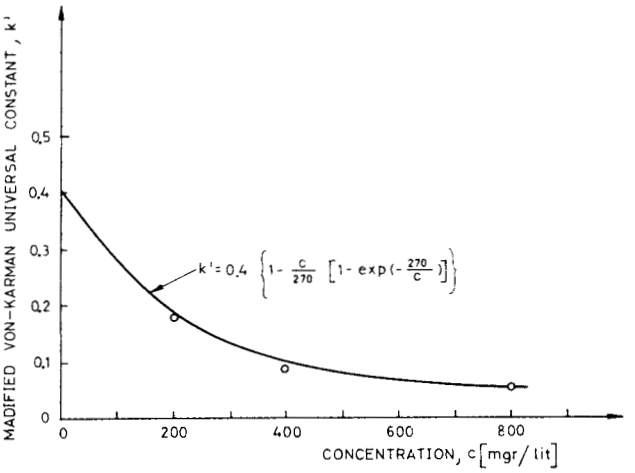

Fig. 9. Modified von Karman universal constant in the grid region.

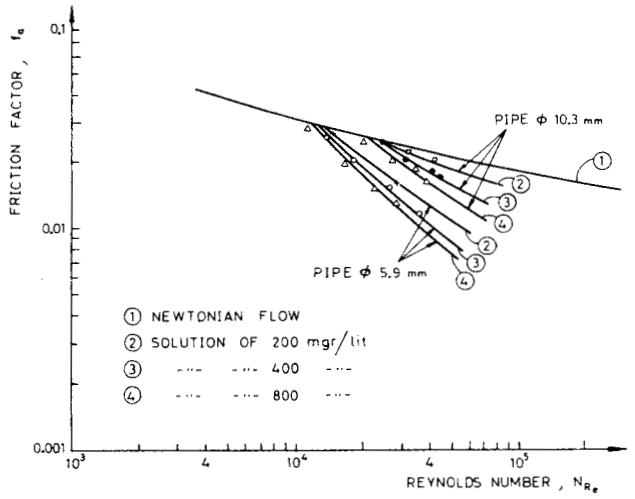

Fig. 7. Turbulent Poiseuille flow of EPR solutions in kerosene.

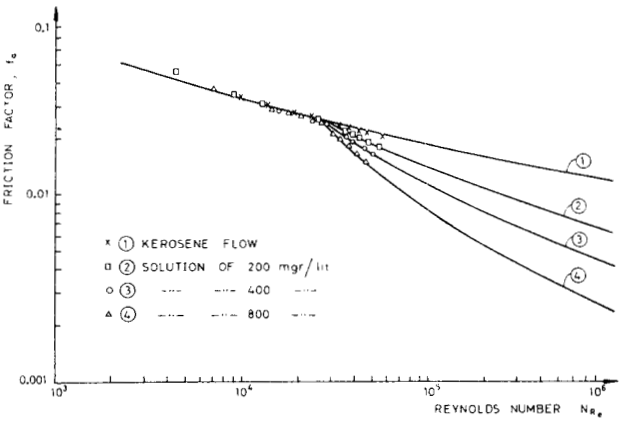

Fig. 10. Comparison between experimental results obtained from annular flow of EPR solutions and computations according to characteristic times approach.

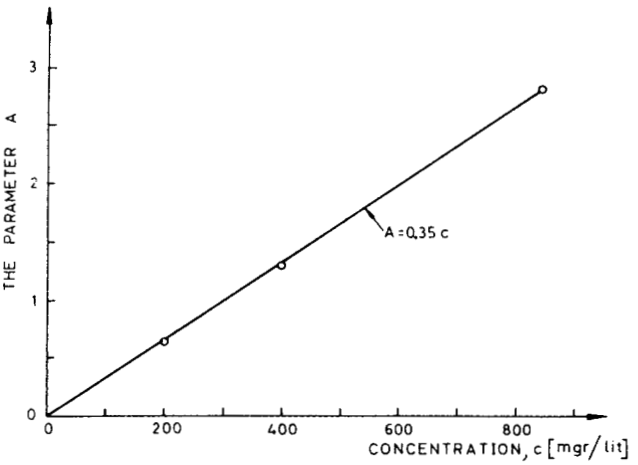

Fig. 8. Description of the constant A as a function of concentrations.

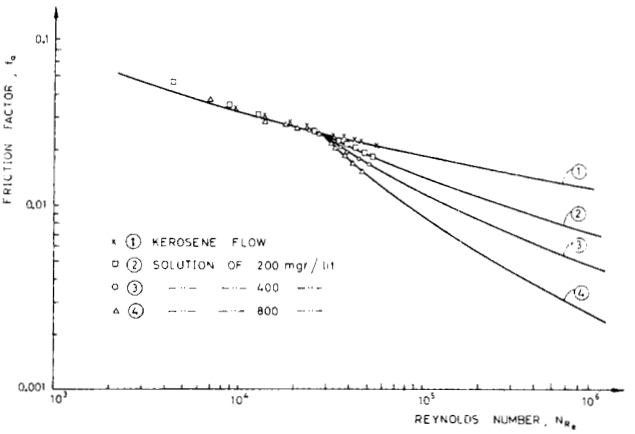

Fig. 11. Comparison between experimental results obtained from annular flow of EPR solutions and computations according to characteristic length approach.

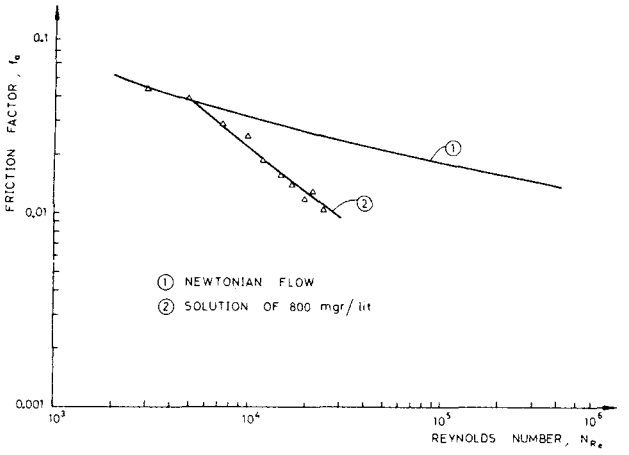

Fig. 12. Experimental results obtained from annular flow of Oppanol solutions.

respectively. In these computations the values of the characteristic times and lengths, as well as the magnitude of A and k', were taken from the pipe flow experiments. The measurements of pressure drop in the annulus system of flowing Oppanol solutions are shown graphically in Figure 12. Here the solid line is based on experimental data only.

CONCLUSIONS

The characteristics of the turbulent flow of dilute polymer solutions may be predicted on the basis of semiempirical relationships which express the variations in velocity profile due to the dissolved polymer. Two such relationships previously developed for pipe flow are identified as the characteristic times approach and the characteristic lengths approach. Using both approaches similar characteristics for annular flow were predicted. A series of experiments with dilute polymer solutions in pipe and annular flow gives results which fit these predictions quite well.

It may be shown that the heat transfer capability through the inner wall of an annular system will be reduced when drag reducing polymers are added to a turbulently flowing solvent. This reduction in heat transfer occurs even when Prandtl number is equal to unity.

ACKNOWLEDGMENT

This research was sponsored by the U.S. Office of Naval Research under Contract N62558-4093 and by the Technion Research Fund.

The authors thank Professor J. L. Zakin from the University of Missouri at Rolla for his helpful comments.

NOTATION

A = parameter depending on the type and concentration of polymeric solution, dimensionless
B = parameter depending on the type of polymeric solution, mg./liter
c = solution concentration, g./ml. or mg./liter
f_a = overall Darcy-Weissbach friction factor as defined in Equation (4), dimensionless
f_1 = Darcy-Weissbach friction factor for core as defined in Equation (4), dimensionless
f_2 = Darcy-Weissbach friction factor for outer wall as defined in Equation (4), dimensionless
k = von Karman's universal constant, dimensionless
k' = modified von Karman's universal constant, dimensionless
L = characteristic length of the polymer, cm.
L^+ = dimensionless characteristic length of the polymer $L\sqrt{\tau_w/\rho}/\nu$
M = molecular weight, g./g.-moles
N_{Re} = Reynolds number as defined in Equation (5), dimensionless
r = radial coordinate, cm.
r_0 = location of maximal local mean velocity, cm.
r_1 = radius of core, cm.
r_2 = radius of outer tube, cm.
R = universal gas constant, erg/°C.
t_1 = maximum relaxation time of the polymer, sec.
T = dimensionless relaxation time as defined in Equation (15), dimensionless
u = local mean velocity, cm.
u^+ = dimensionless local mean velocity $u/\sqrt{\tau_w/\rho}$
u_1^+ = dimensionless local mean velocity at core $u/\sqrt{\tau_{w_1}/\rho}$
u_2^+ = dimensionless local mean velocity at the outer tube $u/\sqrt{\tau_{w_2}/\rho}$
Δu^+ = shift of the logarithmic velocity profile, dimensionless
Δu_1^+ = shift of the logarithmic velocity profile at the core, dimensionless
Δu_2^+ = shift of the logarithmic velocity profile at the outer wall, dimensionless
V_a = average velocity for whole stream, cm./sec.
V_1 = average velocity for inner layer, cm./sec.
V_2 = average velocity for outer layer, cm./sec.
y = distance from the wall, cm.
y^+ = dimensionless distance from the wall $y\sqrt{\tau_w/\rho}$
y_1 = distance from core, cm.
y_1^+ = dimensionless distance from core, $y_1\sqrt{\tau_{w_1}/\rho}/\nu$
y_2 = distance from the outer wall, cm.
y_2^+ = dimensionless distance from outer wall, $y_2\sqrt{\tau_{w_1}/\rho}/\nu$

Greek Letters

$\beta_0 = r_0/r_2$
$\beta_1 = r_1/r_2$
δ = thickness of the laminar boundary sublayer, cm.
δ^+ = dimensionless thickness of the laminar boundary sublayer $\delta\sqrt{\tau_w/\rho}/\nu$
$\lambda = L/r_2$
η = solution viscosity, poise
η_0 = viscosity of the pure solvent, poise
η_{sp} = specific viscosity, dimensionless
θ = absolute temperature, °K.
ν = kinematic viscosity, Stokes
ρ = liquid density, g./cc.
τ_w = shear stress, dyne/sq. cm.
τ_{w_1} = shear stress at the core, dyne/sq. cm.
τ_{w_2} = shear stress at the outer wall, dyne/sq. cm.

LITERATURE CITED

1. Meter, D. M., and R. B. Bird, *AIChE J.*, **7**, 41 (1961).
2. Barrow, H., Y. Lee, and A. Roberts, *Intern. J. Heat Mass Transfer*, **8**, 1499 (1965).
3. Goldstein, S., *Proc. Roy. Soc.*, **A159**, 473 (1937).
4. Macagno, E. O., and P. W. McDougall, *AIChE J.*, **12**, 437 (1966).
5. Meyer, V. A., *LTV Res. Center Rept. No. 0-71000/5R-19* (1965).
6. Elata, C., J. Lehrer, and A. Kahanovitz, *Israel J. Technol.*, **4**, 87 (1966).
7. Hershey, H. C., Ph.D. thesis, Univ. Missouri, Rolla (1965).
8. Virk, P. S., E. W. Merrill, H. S., Micley, K. A. Smith, and E. L. Mollo-Christensen, *J. of Fluid Mech.*, **30**, 305 (1967).
9. Van Driest, E. R., *Ocean System Operations of North American Rockwell Corp. Scientific Rept. AFOSR67-2369* (1967).
10. Rouse, P. E., *J. Chem. Phys.*, **21**, 1272 (1953).
11. Zimm, B. H., *ibid.*, **24**, 269 (1956).
12. Poreh, M., and U. Paz, *Intern. J. Heat Mass Transfer*, **11**, 805 (1968).
13. Pike, M., and W. F. Watson, *Rubber Chem. Technol.*, **26**, 386 (1953).
14. Ram, A., Sc.D. thesis, Massachusetts Inst. Technol., Cambridge (1961).
15. Reiner, M., *Physics Today*, **17**, 62 (1964).

Manuscript received June 9, 1969; revision received October 22, 1969; paper accepted October 27, 1969.